RSC Advances

PAPER

View Article Online
View Journal | View Issue

Cite this: *RSC Adv.*, 2026, **16**, 2767

Highly efficient Cr(VI) removal from water using deep eutectic solvents: a sustainable and comprehensive approach

Thi Nhan Huynh,[ab] Duc Thien Nguyen,[a] Ho Hoang Phuong Uyen Pham,[a] Anh Duc Trinh [b] and Quang Hieu Tran *[c]

Addressing the persistent challenge of hexavalent chromium (Cr(VI)) pollution, this study introduces a sustainable extraction strategy using a novel hydrophobic deep eutectic solvent (HDES) composed of acetic acid and tetraoctylammonium bromide. Under optimized conditions (1 : 4 molar ratio), the HDES exhibited robust extraction capabilities, removing over 95% of Cr(VI) across a broad pH window (2–10). The extraction mechanism was best described by the pseudo-second-order kinetic model, while thermodynamic parameters confirmed a spontaneous and endothermic process ($\Delta H° = 38.21$ kJ mol; $\Delta G° = -16.88$ kJ mol^{-1}). Notably, the method achieved a high enrichment factor of 87-fold in real wastewater samples. The environmental friendliness of the protocol was validated by an AGREE score of 0.76. This work represents the first successful application of an acetic acid-based HDES for Cr(VI) removal, establishing a scalable, efficient, and green methodology for environmental remediation.

Received 11th November 2025
Accepted 31st December 2025

DOI: 10.1039/d5ra08693k

rsc.li/rsc-advances

1. Introduction

Environmental pollution from industrial activities has become increasingly severe. Dyes, nitrophenols, and heavy metals pose significant threats to ecosystems and human health.[1–4] Heavy metals are critical contaminants because of their high toxicity and persistence. These properties compromise ecological integrity and human safety.[5] Therefore, recovering metal ions from industrial and household waste is essential. Recovery reduces environmental contamination and health risks, conserves finite resources, lowers demand for primary mining, and cuts treatment and disposal costs. It also permits recovery of valuable materials for reuse, supporting a circular economy and sustainable resource management. Consequently, researchers have focused on developing novel materials to improve the efficiency, selectivity, and sustainability of metal-ion recovery.[6–10]

Chromium, in particular, is considered a human carcinogen.[11–13] Chromium pollution poses a significant threat to natural resources, especially water and soil.[14] Hexavalent chromium [Cr(VI)] is highly toxic and mobile. It is associated with cardiovascular, developmental, neurological, endocrine, and immunological disorders and with various cancers in humans *via* inhalation and skin contact.[15,16] Due to its harmful effects, Cr(VI) has been designated by the United States Environmental Protection Agency as one of the 129 priority pollutants.[17,18] The World Health Organization (WHO) has identified Cr(VI) as a Group 1 carcinogen, confirming its carcinogenicity to humans[17] To safeguard public health, WHO has set the maximum permissible concentration of total chromium in drinking water at 50 μg L^{-1}. However, studies in the United States and Canada report average Cr(VI) concentrations in drinking water typically between 0.20 and 2.0 μg L^{-1}.[19,20] Therefore, effective methods for reducing Cr(VI) concentrations in aquatic environments are increasingly important. Cr(VI) can be removed from wastewater using various treatment methods such as chemical reduction,[16,21,22] adsorption,[23] and membrane-based filtration techniques.[24] However, conventional techniques for purifying chromium-contaminated aqueous solutions often suffer from limited efficiency and high operational costs. These limitations are particularly problematic when treating trace amounts of chromium.[25] To address these challenges, ionic liquids (ILs) have emerged as eco-friendly alternatives to volatile organic solvents and catalysts due to their low volatility and design flexibility.[26] Nonetheless, certain ILs still pose limitations, including toxicity, complex synthesis procedures, and high production costs.[27]

In recent years, deep eutectic solvents (DESs) have gained attention as promising alternatives to conventional organic solvents. DESs are synthesized by combining hydrogen-bond donors (HBDs) with hydrogen-bond acceptors (HBAs) and are classified into five types (I–V).[28–30] They offer advantages such as low volatility, non-flammability, and high solvation capacity.

[a]*Faculty of Chemistry, Ho Chi Minh City University of Education, 280 An Duong Vuong, Cho Quan Ward, Ho Chi Minh City, 700000, Vietnam*
[b]*Nuclear Training Center, Vietnam Atomic Energy Institute, Hanoi 100000, Vietnam*
[c]*Faculty of Chemical Engineering, Industrial University of Ho Chi Minh City, 12 Nguyen Van Bao, Hanh Thong Ward, Ho Chi Minh City, 700000, Vietnam. E-mail: tg61550280@iuh.edu.vn; hieugodau78@mail.com*

These characteristics render DESs powerful and sustainable media for extraction, separation, and absorption processes.[31–33] Beyond metal recovery, DESs have been widely applied in various green chemistry applications. For example, they are used to extract polyphenols, flavonoids, and alkaloids from plant materials and to efficiently recover pesticides from environmental samples.[34–37] Numerous studies have demonstrated the effectiveness of DESs in metal recovery. For instance, Roldan-Ruiz *et al.* (2020) reported a 94% cobalt recovery from spent lithium-ion batteries using a DES.[38] Similarly, Wang *et al.* (2020) demonstrated a 95% extraction efficiency for lithium and cobalt with a choline chloride–urea DES.[39] DESs based on carboxylic acids and sugars have been shown to extract a wide range of metals with high efficiency.[40,41] In the context of chromium extraction, some studies report extraction efficiencies exceeding 98% for Cr(III) and Cr(VI).[42–44] In our previous research, hydrophobic deep eutectic solvents (HDESs) from fatty acids were used to extract Cr(VI). One HDES achieved a maximum extraction efficiency of 97.4% within 3 min.[45]

To date, there have been no reports on the use of hydrophobic DESs based on acetic acid and tetraoctylammonium bromide for Cr(VI) extraction. Therefore, this study presents a novel green extraction process for removing Cr(VI) from aqueous environments with a high enrichment factor. The method is suitable for both trace-level enrichment and high-concentration removal of Cr(VI), offering high efficiency, environmental compatibility, and potential for broad application. We have thoroughly investigated kinetic properties and thermodynamic parameters; these findings provide valuable insights and open a new approach in environmental remediation. By leveraging DESs' unique properties, this work contributes to green chemical processes that minimize environmental impact while maximizing efficiency.

2. Experimental

2.1. Chemicals and reagents

All chemicals and reagents utilized were analytical grades. Tetraoctylammonium bromide (98%), formic acid (99%), acetic acid glacial (100%), propanoic acid (90%), ethanol (99.45%), acetone (99.5%), acetonitrile (99.5%) and phosphoric acid (85%) were purchased from Merck (Darmstadt, Germany). Potassium dichromate (99%), 1,5-diphenylcarbazide (97%) (DPC), sodium chloride (99.5%), magnesium chloride (99.9%), sodium sulfate (99%), magnesium sulfate (99%), sodium chloride (99%), and sodium hydroxide (99%) were purchased from Xilong (China).

2.2. Instruments

PerkinElmer Lambda 25 was used for scanning the absorption spectra of purple-colored complex. DAIHAN-WiseStir MSH-20D and SK-L330-Pro Large Multifunctional Linear Decolorizing Shaker were used for extraction Cr(VI) in samples.

2.3. Preparation of DESs

Sixteen HDESs were prepared following a procedure adapted from our previous studies with minor modifications.[36,45] The hydrogen bond acceptor, tetraoctylammonium bromide ([N8888]Br), and hydrogen bond donors, including formic acid, acetic acid, propanoic acid, and ethanol, were weighed in molar ratios of 1 : 2, 1 : 3, 1 : 4, and 1 : 6. The mixtures were then heated at 60 °C on a magnetic stirrer for approximately 30 min until homogeneous solutions were obtained. After heating, the solutions were allowed to cool to room temperature and were subsequently stored at ambient conditions for further use.

2.4. Characterization of HDESs

The formation of hydrogen bonds within the DESs was confirmed using Fourier-Transform Infrared (FT-IR) and Nuclear Magnetic Resonance (^{1}H-NMR) spectroscopy. FT-IR spectroscopy was used to identify alterations in the frequency or intensity of characteristic functional group vibrations. Following synthesis, the HDESs were analyzed directly *via* FT-IR using a Thermo Scientific NICOLET iS50 FT-IR spectrometer. Complementary ^{1}H-NMR and NOESY spectroscopy were employed to evaluate chemical shifts of diagnostic signals. These measurements were performed on a Bruker Avance NEO 600 MHz NMR spectrometer.

The thermal stability and phase transitions of the HDESs were evaluated using Thermogravimetric Analysis (TGA) and Differential Scanning Calorimetry (DSC). TGA measurements were conducted on a TGA-550 instrument (TA Instruments, USA) over a temperature range of 30 to 600 °C. DSC analysis was performed using a DSC-250 system (TA Instruments, USA) from 30 to 300 °C. Both analyses were carried out under a nitrogen atmosphere with a constant flow rate of 10 mL min^{-1} to prevent oxidation during heating.

To confirm the presence of chromium and evaluate the elemental distribution within the post-extraction phase, Scanning Electron Microscopy (SEM) mapping coupled with Energy Dispersive X-ray Spectroscopy (EDX) was employed. Prior to analysis, the Cr(VI)-containing HDES samples were solidified at −20 °C for 30 min using a MATOS PLUS Cloud 300F freezer (United Kingdom) to facilitate handling. The solidified samples were then carefully dried to minimize moisture interference, dispersed onto a silicon wafer, and mounted onto an aluminum stub using conductive carbon tape. The analysis was performed using a Hitachi TM4000Plus microscope (Hitachi, Tokyo, Japan) equipped with a Bruker Quantax 75 EDS detector (Bruker, Berlin, Germany). The SEM-EDX acquisition was conducted using an accelerating voltage of 15 kV to ensure sufficient excitation of the characteristic X-ray lines of chromium, with the working distance optimized for maximum X-ray collection efficiency.

2.5. Preparation of standard solutions

A stock solution of diphenylcarbazide (DPC) with a concentration of 0.020 mol L^{-1} was prepared in acetone. Similarly, a stock standard solution of Cr(VI) was prepared by dissolving potassium dichromate ($K_2Cr_2O_7$) in deionized water in a volumetric flask to achieve a concentration of 1000 mg L^{-1}. This stock solution was further diluted with deionized water to prepare a 100 mg L^{-1} standard solution for extraction tests. Calibration standards for Cr(VI) were prepared from the standard solution,

covering a concentration range of 0.10 to 1.0 mg L^{-1}. To form the characteristic, purple-colored Cr-DPC complex, phosphoric acid (H_3PO_4) and DPC were added to all standard solutions.

2.6. Sample collection

Wastewater samples were collected from the wastewater treatment tank of an electroplating factory located in Binh Chanh District, Ho Chi Minh city, Vietnam. The samples were filtered through a 0.6 μm glass fiber filter (Advantec) to remove suspended particles. A filtered sample volume of 1500 mL was collected in a 1500 mL plastic bottle. The sample was then acidified with 0.50 mL of concentrated sulfuric acid (H_2SO_4, 99%) to adjust the pH to approximately 2.

2.7. Extraction procedure

The HDES extraction procedure was based on, with some modifications, the methods reported by Yueyue Shi *et al.*[46] and our previous study.[45] The extraction procedure began by adding 100 mg of HDESs to 10 mL of a 100 mg L^{-1} Cr(VI) solution in a 20 mL vial. The mixture was then shaken for 10 min at 500 rpm to ensure thorough mixing. After the extraction process, the entire aqueous solution was transferred into a 50 mL volumetric flask. To this flask, 0.5 mL of 1.0 M H_3PO_4 solution and 0.25 mL of DPC reagent were added. The mixture was shaken well and made up to the mark with distilled water. The remaining Cr(VI) concentration in the aqueous phase was determined using ultraviolet-visible (UV-vis) absorption spectroscopy at a wavelength of 540 nm, with DPC as the reagent. Upon reaching equilibrium in the extraction process, the extraction efficiency (EE, %), the amount extracted (q_e, mg g^{-1}), the distribution ratio (D), and the enrichment factor (EF) were calculated using the eqn (1)–(4).

$$\mathrm{EE}(\%) = \frac{C_i - C_p}{C_i} \times 100 \quad (1)$$

$$q_e = \frac{(C_i - C_p) \times V_a}{m} \quad (2)$$

$$D = \frac{C_i - C_p}{C_i} \times \frac{V_a}{V_0} \quad (3)$$

$$\mathrm{EF} = \frac{C_0}{C_i} \quad (4)$$

where C_i and C_p (mg L^{-1}) represent the concentrations of Cr(VI) in the aqueous phase before and after extraction, respectively, V_a (mL) is the volume of the initial Cr(VI) solution, V_0 is the volume of HDES, C_0 is the concentration of Cr(VI) in the DES phase, and m (g) represents the mass of the HDES phase.

To evaluate the factors influencing the extraction efficiency of Cr(VI) using HDESs, a series of experiments were conducted. The molar ratio of HBA to HBD was varied at 1 : 1, 1 : 2, 1 : 3, 1 : 4, and 1 : 6 to determine the optimal composition. The effect of shaking time was studied at intervals of 2, 5, 10, 20, 30, and 40 min, while the initial concentration of Cr(VI) was tested at 1, 5, 25, 50, 100, 150, 200, and 250 mg L^{-1}. The influence of temperature was evaluated at 30 °C, 40 °C, and 50 °C, and the pH of the aqueous phase was adjusted to 2, 4, 6, 8, and 10. Additionally, the impact of interfering ions (Na^+, Mg^{2+}, NO_3^-, Cl^-, and SO_4^{2-}) was examined at salt concentrations ranging from 0.2 to 1.0 M to assess their effect on the extraction process.

2.8. Kinetic and thermodynamic studies

To determine the optimal extraction time required to reach equilibrium, a kinetic study was performed. In this study, 0.10 g of HDES was added to 10.0 mL of a Cr(VI) solution (100 mg L^{-1}), and the extraction time was varied (2, 5, 10, 20, 30, and 40 min). The resulting extraction behavior was then analyzed using pseudo-first-order and pseudo-second-order kinetic models. The pseudo-first-order model, which describes extraction rate based on interfacial diffusion, and the pseudo-second-order model, suitable for systems involving chemical interactions like electron or ion exchange,[47,48] were applied to elucidate the rate-limiting step in the Cr(VI) extraction process. These models are expressed by eqn (5) and (6).

To perform a thermodynamic analysis of the extraction process, experiments were conducted at four temperatures: 30 °C, 40 °C, and 50 °C. From these data, the Gibbs free energy change ($\Delta G°$; kJ mol^{-1}), enthalpy change ($\Delta H°$; kJ mol^{-1}), and entropy change ($\Delta S°$; kJ mol^{-1} K^{-1}) were determined. Given the similar temperature dependence of the distribution ratio (D) and the equilibrium constant (K), the Van't Hoff equation was applied using the distribution ratio to estimate $\Delta H°$. Specifically, $\Delta H°$ was derived from the slope of the plot of $\log D$ *versus* $1000/T$. The thermodynamic parameters were then calculated using eqn (7)–(10), as detailed in Table 1.

2.9. Data analysis

The experimental results are presented as means ± standard deviations, calculated from three independent replicates. Microsoft Excel (Office 365) and Origin (Learning version 2024) were used for data visualization and graphical representation. These tools facilitated the processing and refinement of graphs,

Table 1 Kinetic and thermodynamic parameters[a]

Kinetic	Equations
Pseudo-first-order model	$\ln(q_e - q_t) = \ln q_e - k_1 t$ (5)
Pseudo-second-order model	$\frac{1}{q_t} = \frac{1}{k_2 q_e^2} + \frac{1}{q_e t}$ (6)
Thermodynamic	$\ln K = -\frac{\Delta H^\circ}{RT} + \frac{\Delta S^\circ}{R}$ (7)
	$\log D = -\frac{\Delta H^\circ}{RT} + B$ (8)
	$\Delta H° = -2{,}303RT \log D$ (9)
	$\Delta S^\circ = \frac{\Delta G^\circ - \Delta H^\circ}{T}$ (10)

[a] Where q_e and q_t (mg g^{-1}) represent the amount of Cr(VI) ions at equilibrium and at time (t) (min), respectively. The constants (k_1) (1/min) and (k_2) (mg g^{-1} min) denote the rate constants for the pseudo-first-order and pseudo-second-order models, respectively. R is thermodynamic constant (8.314 J mol^{-1} K), T is the absolute temperature (K) and B is integration constant.

diagrams, and spectroscopic data, ensuring a clear and accurate presentation of the findings.

3. Results and discussion

Fig. 1 schematically illustrates the Cr(VI) removal and extraction strategy developed in this work. The process encompasses several key stages, as depicted in the diagram: preparation of the DESs, screening to identify the DES with optimal extraction capability, in-depth characterization of its structure, investigation of factors influencing extraction efficiency, proposition of extraction mechanism, application to real-world samples, and a final assessment of the process's greenness index.

3.1. Preliminary assessment of HDES extraction

The ratio of HBA to HBD plays a critical role in the formation and properties of DES systems. At a 1 : 1 ratio, HDES systems could not be successfully formed, while at HBD ratios of 1 : 2 and 1 : 3, phase formation was challenging, and the synthesized solvents tended to solidify. This phenomenon is primarily attributed to the short carbon chain length of the HBDs, which leads to incompatibility in terms of size and polarity at lower ratios, thereby hindering the formation of a stable liquid phase. Consequently, increasing the HBD ratio is necessary to balance these factors and promote the formation of a stable DES. For HDESs with 1 : 4 and 1 : 6 ratios, the solvents remained in the liquid state at room temperature after synthesis, indicating their structural stability (see more in Table S1). In contrast, for HBDs with long carbon chains, previous studies have demonstrated that DES formation at a 1 : 1 ratio occurs more readily.[44,45]

The extraction capability of the sixteen synthesized DESs in this study was evaluated, as shown in Table 2, all the HDESs demonstrated the ability to nearly completely extract 10 mL of a Cr(VI) standard solution at a concentration of 100 mg L^{-1} with only 0.10 g of DES. Notably, HDESs with 1 : 4 and 1 : 6 ratios retained their liquid state after the extraction process, which facilitates handling and measurement procedures.

Among the four HBDs tested, formic acid and ethanol can act as both reducing agents and neutralizers, which could pose challenges when handling oxidizing samples. While acetic acid is more widely used than propionic acid due to its extensive industrial applications, including in manufacturing, medicine, and daily life. Therefore, considering the balance between extraction efficiency, preparation time, solvent stability, and the availability of HBD, the HDES with a 1 : 4 ratio of CH_3COOH (referred to as HDES 4) was selected for subsequent experiments.

3.2. Characterization of HDES 4

3.2.1. TGA-DSC thermogram. The thermal properties of HDES-4 were studied by TGA and DSC in the temperature range of 40–300 °C under nitrogen (Fig. 2A, B, S1, and S2). The DSC curve showed three clear endothermic peaks. The first peak appeared at around 120 °C with an enthalpy of 78.5 ± 0.9 J g^{-1}, followed by a second one at 131 °C with an enthalpy of 76.1 ± 1.1 J g^{-1}. These two close events can be explained by the evaporation of free or weakly bound acetic acid and the release of residual water. The energy values indicate that these processes consume a moderate amount of heat, suggesting that the interactions between the acetic acid molecules and the ionic matrix are relatively weak. The third and most significant endothermic transition was observed at 208 °C with a much larger enthalpy of 269.4 ± 2.2 J g^{-1}. In agreement, the DTG curve revealed two mass-loss peaks at 190 °C and 208 °C, supporting the DSC data and confirming that these transitions correspond to the evaporation of more strongly bound acetic acid and the onset of quaternary ammonium cation

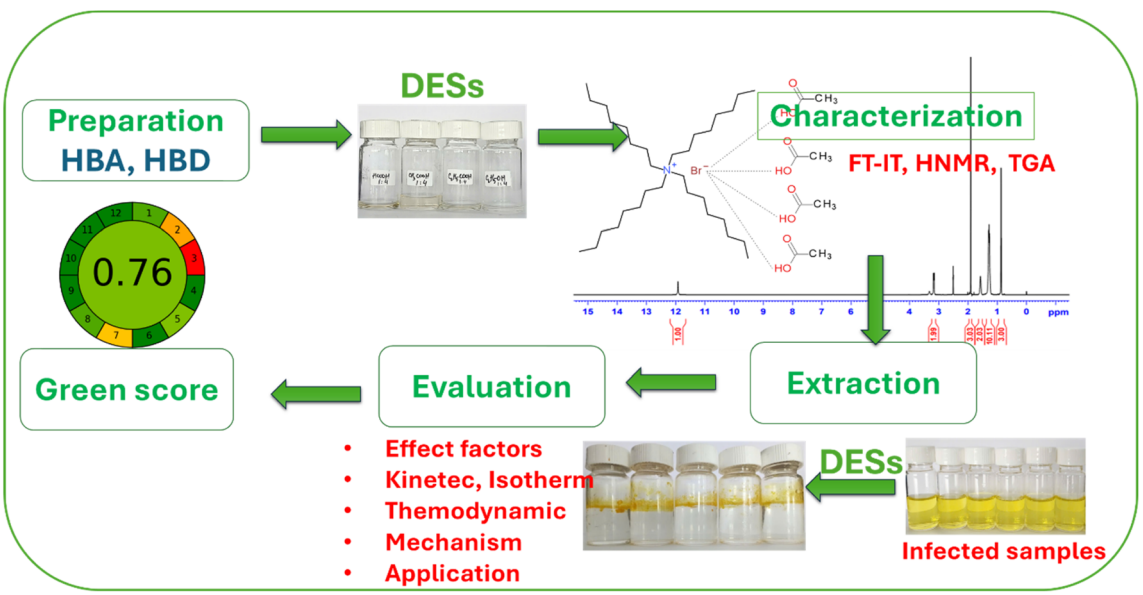

Fig. 1 Schematic illustration of chromium hexavalent extraction strategy in this work.

Table 2 Comparative Cr(VI) extraction efficiencies of HDESs ($n = 3$)

HBA	Mole ratio	HBD, EE, %			
		HCOOH	CH_3COOH	C_2H_5COOH	C_2H_5OH
[N8888]Br	1 : 1	—	—	—	—
	1 : 2	98.66 ± 1.05	99.57 ± 1.21	99.40 ± 0.98	93.73 ± 1.33
	1 : 3	99.06 ± 1.23	98.98 ± 1.42	99.12 ± 1.32	98.57 ± 1.40
	1 : 4	99.07 ± 1.30	99.19 ± 2.24	99.32 ± 1.39	98.34 ± 2.22
	1 : 6	99.49 ± 2.09	99.21 ± 2.10	99.24 ± 1.23	98.94 ± 3.56

decomposition. This thermal behavior is consistent with previous studies on quaternary ammonium-based DESs, which reported decomposition temperatures in the range of 200–250 °C.[49–51] The large enthalpy value highlights that stronger hydrogen-bonded networks require much more energy to break, confirming the non-uniform binding strength within the HDES structure.

These thermal events were consistent with the TGA results. The sample mass stayed nearly constant up to 100 °C. Between 100 and 160 °C, a gradual mass loss of about 18.5% occurred, matching the two smaller DSC peaks. A sharp weight loss of 81.5% was observed between 160 and 220 °C, which corresponds to the large DSC endotherm at 208 °C. Above 230 °C, the sample was almost completely volatilized, leaving negligible residue in nitrogen. This indicates that the HDES evaporates and decomposes cleanly, without forming char or solid residue.

Thus, HDES-4 is thermally stable only up to approximately 110 °C. Above this point, significant acetic acid evaporation begins, and the material quickly loses stability. For practical applications, the safe operating temperature is below 120 °C. The enthalpy data clearly show that weaker hydrogen-bonded acetic acid leaves the system at lower temperatures with modest energy input, while strongly bound acid and ionic species require much higher energy, leading to sharp decomposition at higher temperatures. This highlights the key role of hydrogen-bond strength distribution in controlling both the volatility and thermal stability of HDES systems.

3.2.2. FT-IR, ^{1}H-NMR and NOESY spectrum. The analysis of the IR spectra provides compelling evidence for the successful formation of the HDES 4 from the hydrogen bond donor CH_3COOH, and the hydrogen bond acceptor [N8888]Br (Fig. 2C). The IR spectrum of the HBA reveals the presence of long alkyl chains through sharp C–H stretching vibrations (3000–2800 cm^{-1}) and bending vibrations (1470–1450 cm^{-1} and 1375 cm^{-1}), while the absence of a distinct C–Br peak confirms the presence of bromide in its ionic form. Conversely, the IR spectrum of the HBD (CH_3COOH) exhibits a broad O–H stretching band (3300–2500 cm^{-1}), indicative of strong hydrogen bonding between carboxylic acid molecules, along with a sharp C=O stretching band and characteristic C–O stretching and bending vibrations, further confirming the presence of the carboxyl group.

The formation of HDES 4 is substantiated by significant changes in the IR spectrum compared to the starting materials. Specifically, the broadening and shifting of the O–H stretching band indicates enhanced hydrogen bonding within the DES due to interactions between acetic acid and the bromide anion. Alterations in the position and shape of the carbonyl stretching band further suggest a modified environment surrounding the

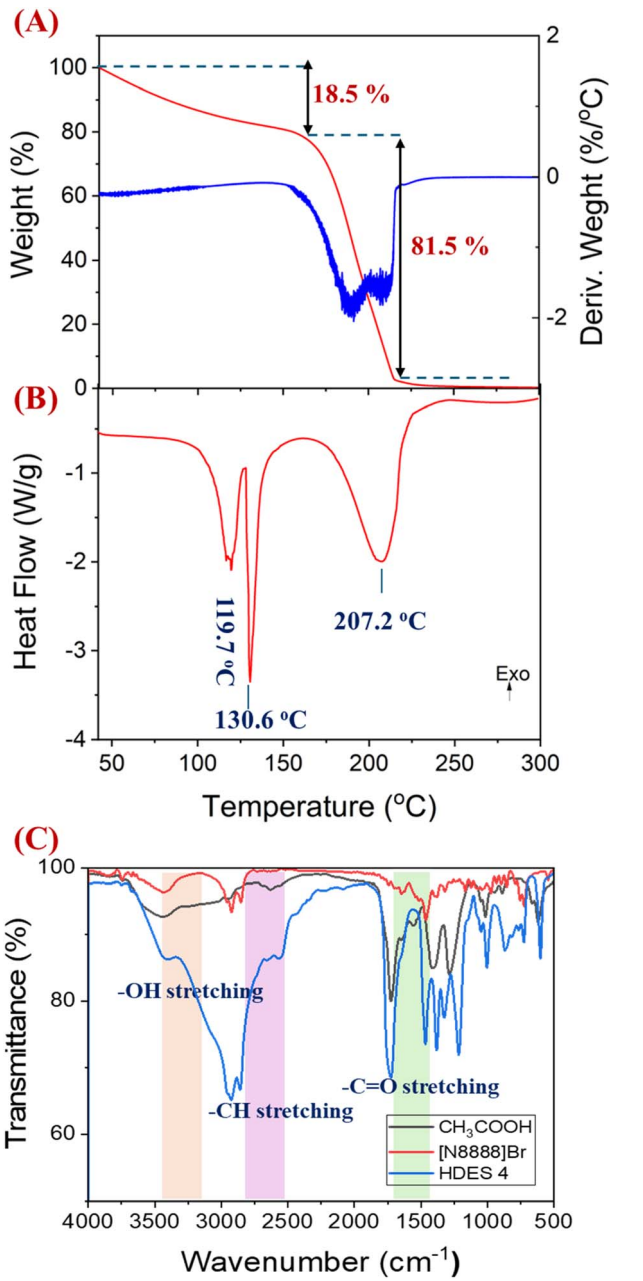

Fig. 2 TGA (A) and DSC (B) behavior, and FT-IR spectrum (C) of HDES 4.

carbonyl group due to DES formation. Furthermore, the persistence of peaks associated with the alkyl chains of [N8888]Br confirms its structural incorporation into the DES.

In summary, the functional groups within the HBA and HBD interact to create a novel DES structure with distinct spectroscopic characteristics. The evidence from the IR spectra, particularly the broadening and shifting of the O–H stretching band in conjunction with alterations in the carbonyl region, provides convincing support for the successful formation of HDES 4. This comprehensive analysis, grounded in the characteristic vibrations of functional groups, highlights the crucial role of hydrogen bonding in the generation of this DES.

The successful preparation of the HDES 4 is confirmed by the combined analysis of its NMR and NOESY spectra, alongside the NMR spectra of its individual components. The ^{1}H-NMR spectrum of [N8888]Br (Fig. 3A and Table S2) displays characteristic signals for the tetraoctylammonium cation: δ = 0.871 ppm (H_a, methyl protons), δ = 1.277 ppm (H_b, $(CH_2)_5$ methylene protons), δ = 1.577 ppm (H_c, methylene protons), and δ = 3.184 ppm (H_d, N–CH_2 protons). The ^{1}H-NMR spectrum of acetic acid (Fig. 3B) exhibits a methyl proton signal at δ = 1.91 ppm and a carboxylic acid proton signal at δ = 11.913 ppm. The ^{1}H-NMR spectrum of HDES 4 (Fig. 3C) combines features of both components, with $[N8888]^+$ signals largely unchanged and the methyl group signal from acetic acid present at δ = 1.91 ppm. Crucially, the slight downfield shift of the carboxylic proton from δ = 11.913 (acetic acid) to 11.921 ppm (HDES 4), providing strong evidence for specific interactions between acetic acid and [N8888]Br. Although the change is small (0.008 ppm), the carboxylic proton is highly sensitive to local electronic environments. The observed deshielding effect is consistent with hydrogen bonding between the acidic proton and the bromide anion, which withdraws electron density from the –COOH group. In addition, the bulky $[N8888]^+$ cation may stabilize this interaction by creating a less polar microenvironment, thereby enhancing the strength of the hydrogen bond.

To solidify this conclusion, the NOESY spectrum provides vital spatial information (Fig. 4). The presence of cross-peaks between the N–CH_2 protons of [N8888]Br (δ = 3.184 ppm) and the carboxylic acid proton of acetic acid (δ = 11.921 ppm) confirms that these groups are in close spatial proximity, definitively indicating a strong interaction between the components in the HDES 4. Furthermore, cross-peaks between the alkyl chain protons of [N8888]Br (δ = 0.871–1.577 ppm) and acetic acid protons offer additional support. Therefore, the retention of characteristic signals from [N8888]Br, the diminishing of the carboxylic acid proton signal in the HDES 4 spectrum, and the presence of key N–CH_2/carboxylic acid cross-peaks in the NOESY spectrum, collectively demonstrate the formation of a DES through a strong, spatially defined

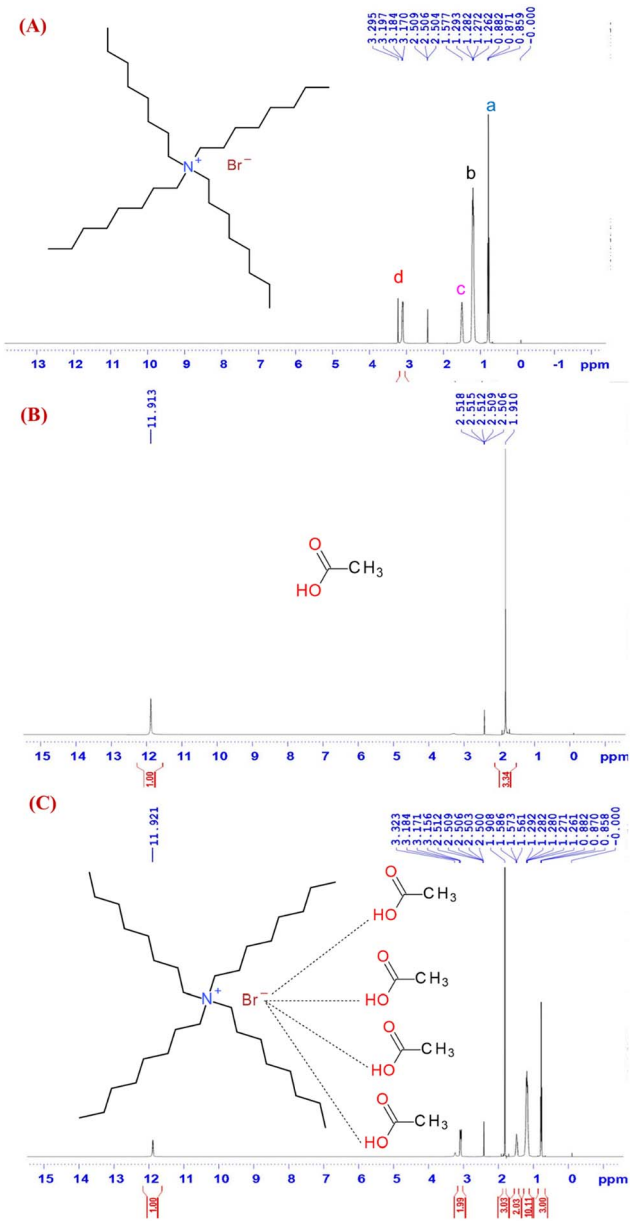

Fig. 3 ^{1}H-NMR spectrum of HBA (A), HBD (B), HDES 4 (C) in DMSO-d_6.

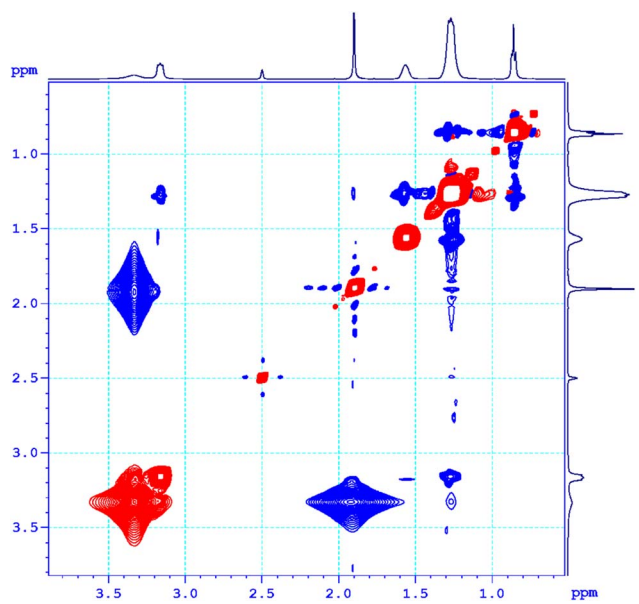

Fig. 4 NOESY spectrum of HDES 4.

interaction between the HBA and HBD, with hydrogen bonding playing a critical role. These findings confirm the successful synthesis of a DES composed of tetraoctylammonium bromide and acetic acid.

3.3. Factors affecting extraction efficiency of HDES 4

3.3.1. Method validation for Cr(VI) quantification. In this study, we quantified Cr(VI) in both aqueous and HDES 4 matrices. To ensure the accuracy and reliability of our results across these different sample types, we validated the method in both matrices.

For the aqueous matrix, Cr(VI) was quantified using the DPC reagent, which forms a colored complex directly in the water. To thoroughly validate the method's performance for aqueous samples, we evaluated the range and linearity, limit of detection (LOD), limit of quantification (LOQ), precision, and stability of the resulting Cr–DPC complex. LOD and LOQ were assessed using the standard formulas LOD = $3\sigma/a$ and LOQ = $10\sigma/a$, where σ is the standard deviation of a series of blanks and a is the slope of the calibration curve. The calibration curve was constructed over the Cr(VI) concentration range 0.1–1.0 mg L^{-1} and yielded the equation Abs = $(0.5661 \pm 0.0206)x + (0.0227 \pm 0.0045)$, $R^2 = 0.9947$ (Fig. 5). The LOD and LOQ for the method were determined to be 0.03 mg L^{-1} and 0.10 mg L^{-1}, respectively (see more details in Table S3). To assess repeatability, three Cr(VI) standards with concentrations of 0.10, 0.50, and 1.0 mg L^{-1} were measured in triplicate, resulting in relative standard deviations (RSDs) ranging from 1.9% to 2.9% ($n = 3$).

For the HDES matrix, the 0.10 g HDES 4 was completely dissolved in 50 mL acetonitrile, and the quantification procedure followed the same protocol as that used for the aqueous matrix. Method validation in the DES matrix yielded a limit of detection (LOD) of 0.04 mg L^{-1} and a linear range from 0.1 to 1.0 mg L^{-1} (see more details in Table S4). The regression equation for the calibration curve was $y = (0.4457 \pm 0.007)x + (0.03511 \pm 0.00139)$ ($R^2 = 0.9905$), with recovery rates exceeding 95%, relative standard deviations ranging from 2.2% to 3.9% ($n = 3$). A comparison of the linear calibration curve slopes between the aqueous and DES matrices, as well as the LOD values, indicates a higher sensitivity in the aqueous phase. This suggests a slight matrix effect from the DES phase that influences optical absorbance at the measured wavelength. However, with an LOD of 0.04 mg L^{-1}, trace chromium detection remains feasible. Furthermore, the post-extraction DES phase is highly enriched in chromium, ensuring that quantification is not hindered. These validation parameters collectively confirm the suitability of the method for Cr(VI) quantification in both aqueous and HDES matrices.

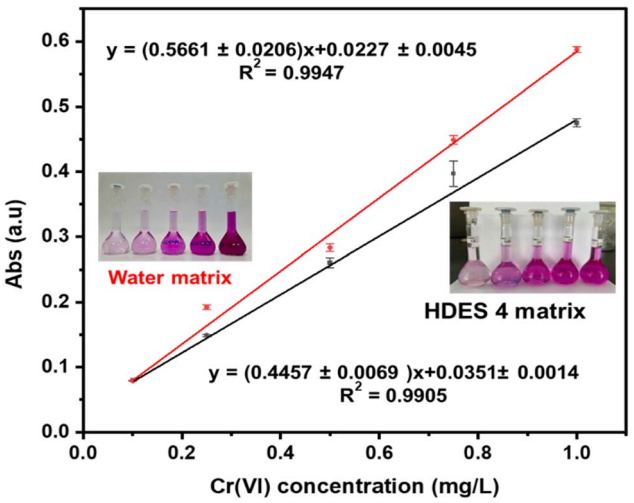

Fig. 5 Calibration curves of Cr(VI)-DPC complex in water matrix (orange curve) and in HDES 4/acetonitril matrix (black curve). Error bars represent the standard deviation of three independent replicates ($n = 3$).

3.3.2. Effect of pH of aqueous phase. The pH of a solution is a critical parameter influencing the extraction efficiency of heavy metal ions. While metal ion solubility and extractant effectiveness are often pH-dependent.[52] The speciation of the target metal itself can also play a significant role. In the case of Cr(VI), the pH of the solution is crucial in determining the prevalent ionic species, directly impacting extraction efficiency.[53] In acidic environments, Cr(VI) predominantly exists as $HCrO_4^-$ and $Cr_2O_7^{2-}$, resulting in an orange solution. Conversely, in alkaline conditions, Cr(VI) primarily manifests as CrO_4^{2-}, leading to a yellow solution.[54] To investigate the effect of pH on Cr(VI) extraction using HDES 4, a series of experiments were conducted. Specifically, 100 mg of HDES 4 was added to 10 mL of a Cr(VI) standard solution (100 mg L^{-1}) at varying pH levels (2, 4, 6, 8, and 10), adjusted using phosphoric acid and sodium hydroxide. Following extraction and quantification of Cr(VI) in the aqueous phase according to the procedure outlined in Section 2.3, the results, depicted in Fig. 6A, indicate that the HDES 4, derived from acetic acid, effectively extracts nearly all Cr(VI) from the 10 mL standard solution across the entire pH range tested (pH 2–10). This suggests that the inherent acidity of the HDES 4 is conducive to the extraction process, likely facilitated by an ion exchange mechanism between bromide ions and $HCrO_4^-$ ions ($pK_a = 6.5$). The pH-independent extraction efficiency is advantageous for the recovery of Cr(VI) from real-world samples, eliminating the need for a preliminary pH adjustment step.

3.3.3. Effect of shaking time. The effect of shaking time on the Cr(VI) extraction efficiency of the acetic acid-derived deep eutectic solvent was investigated, and the results are presented in Fig. 6B. Initially, increasing the shaking time increased the extraction efficiency. However, after 10 min, the efficiency plateaued, reaching values between 98.24% and 98.93% with no significant further improvement. This equilibration time is longer than that observed in some previous studies; for example, Dong *et al.* achieved equilibrium within 2 min using a C6-based DES,[44] and we observed equilibration within approximately 1.0 min using a C16-based HDES.[45] This difference may be attributed to the lower carbon number and higher polarity of the HBD used in this study. Therefore, a shaking time of 10 min was selected as the standard condition for subsequent experiments.

3.3.4. Effect of Cr(VI) concentration. Fig. 6C demonstrates high Cr(VI) extraction efficiency using HDES 4 across

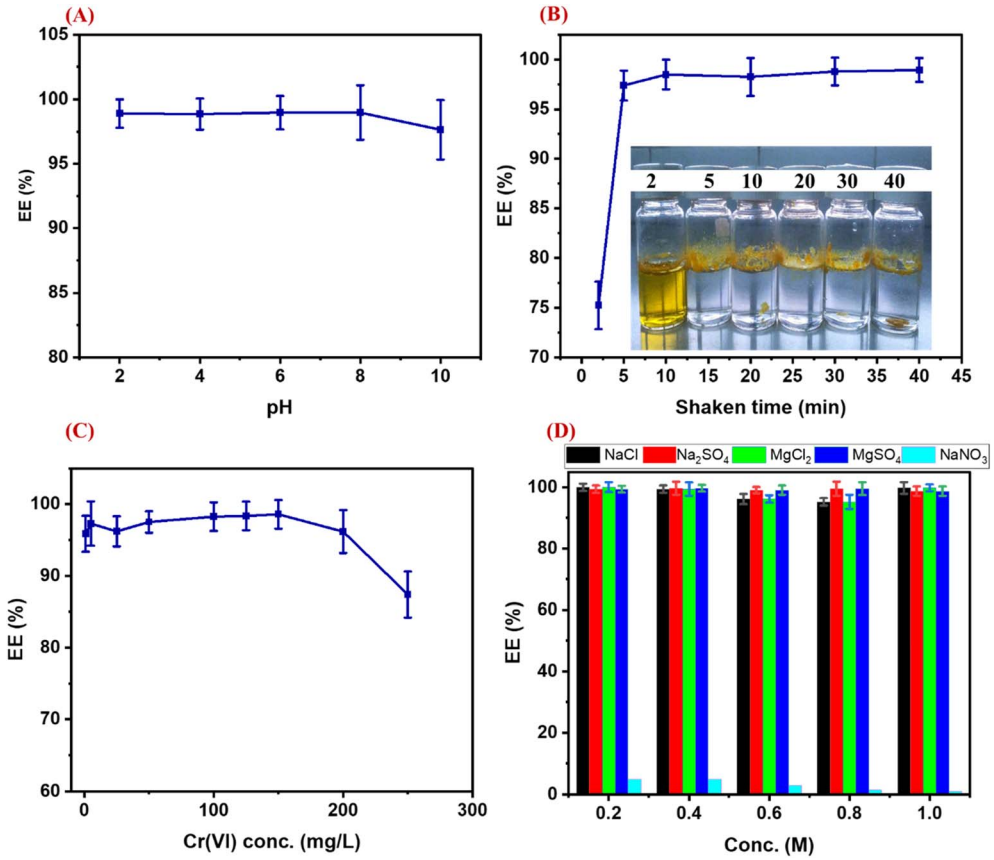

Fig. 6 Influence of various factors on Cr(VI) extraction efficiency: (A) pH, (B) shaking time, (C) initial Cr(VI) concentration (1.0–250 mg L^{-1}), and (D) interfering ions. Error bars represent the standard deviation of three independent replicates ($n = 3$). General experimental conditions: 100 mg HDES 4, 10 mL Cr(VI) solution (100 mg L^{-1}), room temperature, and natural pH (unless varied as a parameter).

a concentration range of 1.0 to 250 mg L^{-1}. This indicates that within this concentration range, the HDES 4 effectively removes virtually all of the Cr(VI) from the aqueous phase. However, when the initial Cr(VI) concentration exceeds 200 mg L^{-1}, a decrease in extraction efficiency is observed, suggesting that the extraction capacity of the HDES 4 for Cr(VI) is being saturated. This saturation effect could stem from several factors, including a limited number of available binding sites for Cr(VI) species within the HDES 4, increased viscosity hindering mass transfer, an unfavorable shift in the equilibrium between the aqueous and organic phases, or the presence of competing anions Br^-.

3.3.5. Effect of interfering ions. Evaluating the influence of salt ions on metal ion extraction is crucial for several reasons.[55] First, these ions can compete with the target metal ions for binding sites on the extractant, potentially reducing recovery efficiency. Second, salt ions can alter the solubility and ionic state of the metals themselves, influencing their extractability. Finally, and perhaps most importantly, investigating salt ion effects enhances the representativeness of the extraction process in relation to real-world environmental samples, which often contain high and variable salt concentrations. This allows for a more accurate assessment of the extraction method's stability and effectiveness under practical conditions. Interfering ions are one of the factors that need to be considered because they can affect the selectivity/specificity of the analytical method.[52,56] Weigh the masses of NaCl, $MgCl_2$, Na_2SO_4, $MgSO_4$ salts and dissolve them in 10 mL of Cr(VI) standard solution with a concentration of 100 mg L^{-1}. As illustrated in Fig. 6D, ions such as chloride, sulfate, sodium, and magnesium in the aqueous phase exhibit negligible impact on solvent extraction efficiency, even at concentrations up to 1.0 M. Furthermore, these ions are unlikely to reach such high concentrations in real-world samples as those tested. Notably, the presence of nitrate anions significantly impacts the extraction process of HDES 4. Specifically, at a nitrate concentration of 0.2 M, the extraction of Cr(VI) is almost completely inhibited, resulting in an extraction efficiency approaching zero. This negative effect of nitrate ions on the extraction capabilities of deep eutectic solvents has been observed and reported in our previous work,[45] as well as by other researchers in the field. According to these studies, a major factor contributing to this effect is the significantly negative standard Gibbs free energy of hydration ($\Delta hydG^\circ$) for NO_3^-, with reported values of -300 kJ mol^{-1}. This contrasts with values for SO_4^{2-}, and Cl^- hydration processes, which are approximately -1080 and -340 kJ mol^{-1}, respectively.[57,58] This suggests that the strong hydration of nitrate ions hinders their interaction with the DES, impeding the extraction of Cr(VI). Potential mitigation strategies could involve the use of adsorbents, such as activated carbon, to

remove nitrate ions, or reduction methods employing Devarda's alloy or cadmium columns to convert nitrate to ammonium or nitrite ions. However, further experimental investigation is required to effectively address this issue. In reality, nitrate concentrations rarely reach such high levels in real-world scenarios.

3.4. Kinetic and thermodynamic analysis

3.4.1. Kinetic analysis. The extraction kinetics of Cr(VI) were analyzed using both pseudo-first-order and pseudo-second-order models. As presented in Fig. 7A, B and Table 3. The pseudo-first-order model yielded an experimental equilibrium adsorption capacity $q_{e,exp}$ of 10.35 ± 0.32 mg g^{-1}, while the calculated value $q_{e,cal}$ was 3.45 ± 0.21 mg g^{-1}, with a rate constant K_1 of 0.1550 ± 0.0271/min and a correlation coefficient R^2 of 0.8911. This relatively low R^2 value suggests that the pseudo-first-order model does not adequately describe the extraction process. In contrast, the pseudo-second-order model showed a much better fit, with $q_{e,cal}$ at 10.49 ± 0.11 mg g^{-1}, which is very close to the experimental value. The constant rate of K_2 was 0.18 ± 0.05 g mg^{-1}. min, and the correlation coefficient R^2 was 0.9998. This high R^2 value and the close agreement between $q_{e,exp}$ and $q_{e,cal}$ indicate that the pseudo-second-order model is more suitable for describing the extraction kinetics of Cr(VI) by HDES 4.

Extraction (or adsorption) capacity depends on multiple factors, including the material's intrinsic properties, the operating environment, and the nature of the target ion. For HDESs, capacity is strongly influenced by composition and structure, particularly the hydrogen-bond donor (HBD). For example, Dong (2024) reported Cr(VI) extraction capacities for HDESs containing C6, C8, C10, and C12 fatty acids in the range 44.81–49.84 mg g^{-1}.[44] In our previous work, an HDES prepared from tetraoctylammonium bromide (N8881Br) and palmitic acid exhibited a Cr(VI) adsorption capacity of 48.3 mg g^{-1}.[45] By contrast, many solid-phase materials show substantially higher capacities. An organic ligand-based sustainable composite hybrid material (CMH) exhibited a lutetium(III) adsorption capacity of 171.76 mg g^{-1}.[59] *N*,*N*-Bis(salicylidene)-1,2-bis(2-aminophenylthio)ethane (BSBAE) was synthesized and grafted onto mesoporous silica to fabricate an optical composite material (OCM), which showed a Cd(II) adsorption capacity of 179.65 mg g^{-1}.[60] Mesoporous silica materials have also demonstrated high capacities for nickel, with reported adsorption of 199.19 mg g^{-1}.[61]

Table 3 Kinetic and isotherm of Cr(VI) extraction (n = 3)

$q_{e,exp}$ mg g^{-1}	$q_{e,cal}$ mg g^{-1}	K_1 1/min	R^2
Pseudo-first-order			
10.35 ± 0.32	3.45 ± 0.21	0.1550 ± 0.0271	0.8911
$q_{e,exp}$ mg g^{-1}	$q_{e,cal}$ mg g^{-1}	K_2 g mg^{-1} min^{-1}	R^2
Pseudo-second-order			
10.35 ± 0.32	10.49 ± 0.11	0.18 ± 0.05	0.9995

3.4.2. Thermodynamics of the extraction process. The thermodynamic analysis not only provides a deeper understanding of the extraction mechanism but also offers valuable insights for scaling up the process under varying thermal conditions. The thermodynamics of the extraction process provides essential insights into the interaction between Cr(VI) ions and the HDES 4. As illustrated in Fig. 6C, HDES4 exhibited remarkable extraction performance at room temperature, achieving efficiencies exceeding 95% within the analyte concentration range of 1–200 mg L^{-1}. However, when the concentration was increased to 250 mg L^{-1}, a decline in extraction efficiency was observed, reaching approximately 86%. This decrease is likely related to the saturation of the extractant phase, where the limited availability of active sites and reduced solute diffusion hinder the mass transfer of analyte molecules. Temperature is another critical parameter influencing extraction efficiency through its effects on solvent viscosity, solute solubility, and interfacial mass transfer. To further clarify this relationship, experiments were conducted at a solute concentration exceeding the saturation level of HDES 4 at 250 mg L^{-1}. The extraction efficiency of Cr(VI) was evaluated at different temperatures (30 °C, 40 °C, and 50 °C). The results, as shown in Table S5, indicated a slight increase in extraction

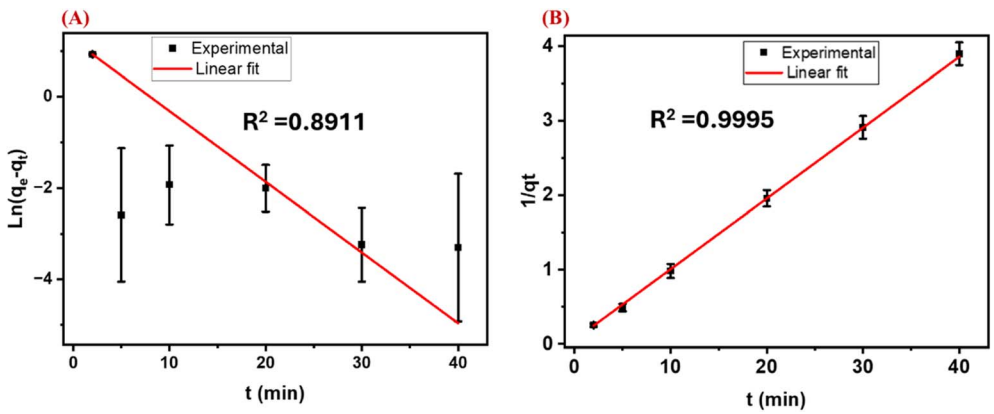

Fig. 7 Kinetic and Isotherm models fitted to Cr(VI) extraction data: (A) pseudo-first-order kinetic model, (B) pseudo-second-order kinetic model. Data represent Cr(VI) extraction (1.0–250 mg L^{-1}) using HDES 4. Error bars indicate the standard deviation of three independent replicates (n = 3).

Table 4 The thermodynamic parameters for Cr(VI) extraction at different temperatures ($n = 3$)

T(K)	$\Delta G°$ (kJ mol^{-1})	$\Delta H°$ (kJ mol^{-1})	$\Delta S°$ (kJ mol^{-1} K)	R^2
303.15	−16.88 ± 0.98	38.21 ± 0.92	0.1817 ± 0.018	0.9840
313.15	−24.4 ± 1.02		0.1999 ± 0.032	
323.15	−26.18 ± 0.45		0.1993 ± 0.021	

efficiency with rising temperature, suggesting that the process is endothermic.

To further understand the extraction mechanism, the thermodynamic parameters, including Gibbs free energy change ($\Delta G°$), enthalpy change ($\Delta H°$), and entropy change ($\Delta S°$), were calculated. As shown in Table 4, the positive value of $\Delta H°$ (38.21 ± 0.92 kJ mol^{-1}) confirms that the extraction process requires energy, which is consistent with the endothermic nature of the reaction. This energy overcome the energy barrier for the separation of DES molecules and promote the formation of ionic interaction with the $HCrO_4^-$ ions in the aqueous phase.

The positive value of $\Delta S°$ (0.1817 ± 0.018 kJ mol^{-1} K) indicates an increase in the system's disorder during the extraction process, which is favorable for the spontaneous nature of the reaction. The negative value of $\Delta G°$ (−16.88 ± 0.98 kJ mol^{-1} at 303.15 K) further confirms that the extraction of Cr(VI) by HDES 4 is a spontaneous process. The decrease in $\Delta G°$ with increasing temperature suggests that higher temperatures enhance the extraction efficiency, making the process more favorable under elevated thermal conditions. The coefficient of determination ($R^2 = 0.9840$) indicates a good fit of the experimental data to the thermodynamic model, reinforcing the reliability of the calculated parameters. These findings align with our previous research[45] and are supported by studies from other authors,[44] reinforcing the conclusion that temperature plays a significant role in optimizing the extraction of Cr(VI) using DES. Although, the extraction efficiency exhibited a slight increase, rising from 96.4% to 98.9%, as the temperature was elevated from 298.15 K to 328.15 K. However, this marginal improvement indicates that temperature exerts only a minimal influence on the overall extraction performance. Given this observation, it is practical to carry out the Cr(VI) removal process at room temperature in real-world water treatment applications, as it offers a balance between efficiency and energy conservation.

3.5. Proposed extraction mechanism

To confirm the presence of chromium in the organic phase, the HDES 4-Cr(VI) extract was analyzed using SEM-EDX mapping. Fig. 8A illustrates the energy-dispersive X-ray spectrum of the extract, revealing the presence of elements consistent with the solvent composition, including C, N, and O, along with Cr. This confirms the successful extraction of Cr(VI) from the aqueous solution by the deep eutectic solvent. Fig. 8B presents the

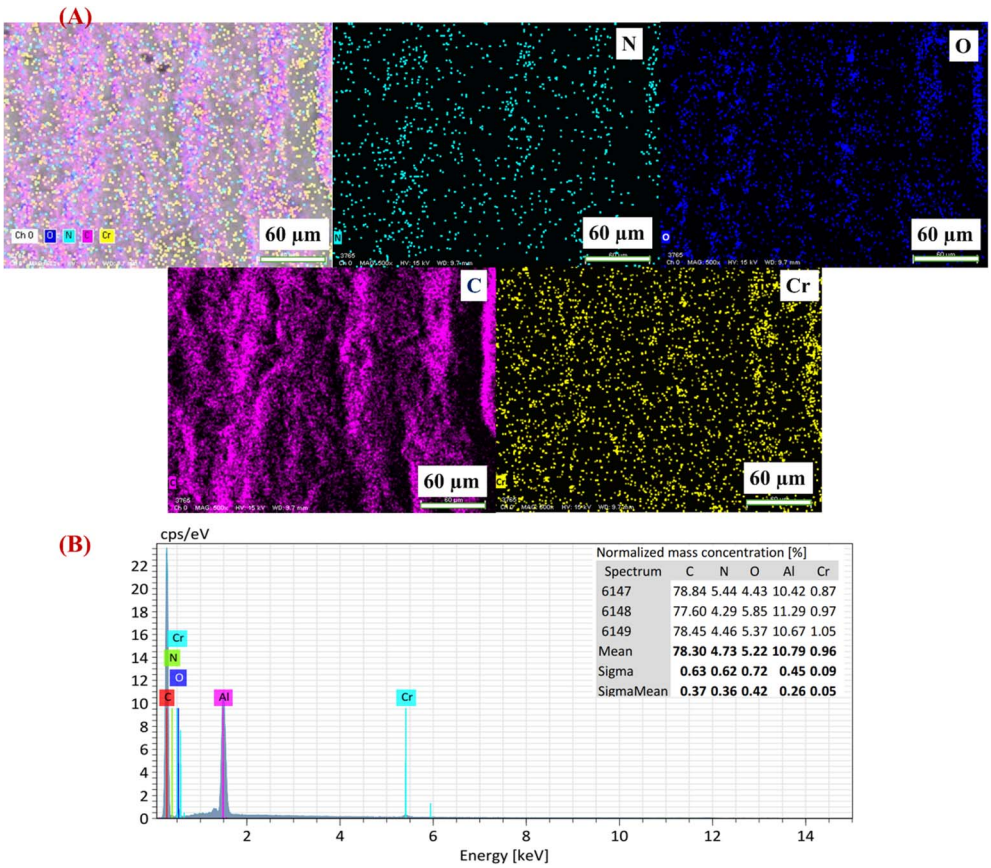

Fig. 8 (A) SEM-EDX mapping and (B) elemental analysis of HDES 4-Cr(VI) after extraction.

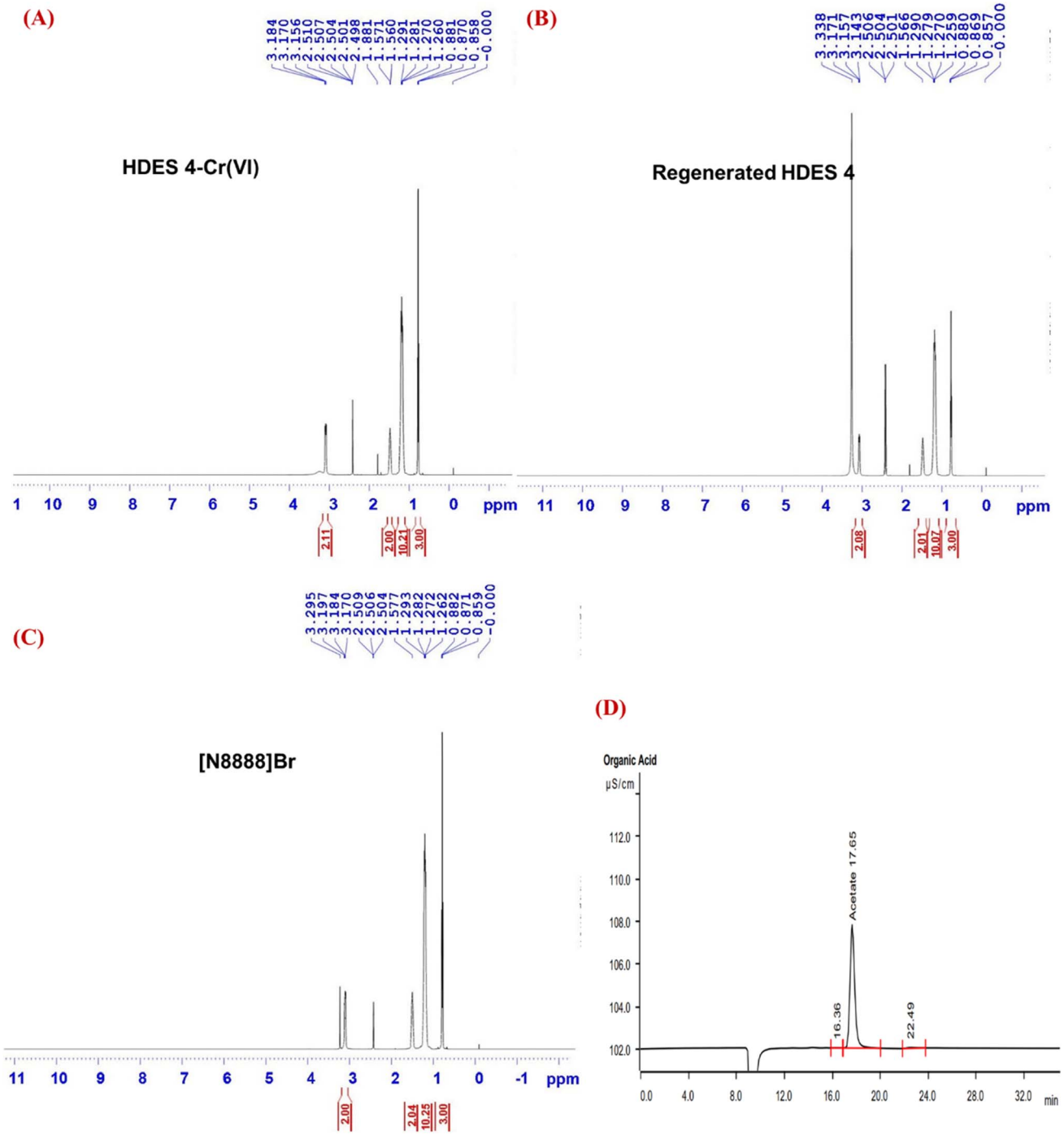

Fig. 9 ^{1}H-NMR of HDES 4-Cr(VI) (A), Regenerated HDES 4 (B), [N8888]Br (C), and IC chromatogram of standard of acetate (D).

elemental composition and weight percentages of the Cr-containing HDES 4 extract, showing a chromium weight percentage of 0.92%.

Additionally, ^{1}H-NMR spectroscopy was employed to further characterize the structure of HDES 4-Cr(VI) and the regenerated HDES 4 (Fig. 9A and B). The ^{1}H-NMR spectra of both HDES 4-Cr(VI) and the regenerated HDES 4 (obtained by soaking in 1.0 M KBr solution for 2 hours, followed by washing and drying) no longer exhibited the characteristic peaks of acetic acid. A comparison of the ^{1}H-NMR spectrum of regenerated HDES 4 (Fig. 9B) and that of [N8888]Br (Fig. 9C) revealed a high degree of similarity in chemical shifts. Specifically, the chemical shift values were largely consistent; the multiplet corresponding to the $-CH_2-$ group adjacent to nitrogen shifted slightly from 3.295 ppm in the [N8888]Br sample to 3.338 ppm in the regenerated sample. While most other signals were nearly identical between the two samples, suggesting minimal structural changes, these findings indicate that the elution process with KBr resulted in the release of CH_3COOH into the aqueous phase, effectively restoring the original HBA.

To confirm this assertion, we quantified the acetic acid released into the aqueous phase using both titration and ion exchange chromatography. For the titration method, 10 mL of the aqueous solution required 5.95 mL of 0.085 M NaOH solution to reach the equivalence point. This indicated the presence of 0.50575 mmol of CH_3COOH, closely matching the 0.50326 millimoles of CH_3COOH present in 0.1 grams of the initial HDES 4. For the ion chromatography (IC) analysis, the method was performed using a Metrohm 850 Professional IC system (Switzerland). Separation was achieved using a Metrosep Organic Acids 250/7.8 analytical column combined with a Metrosep Organic Acids Guard/4.6 guard column, employing a conductivity detector. The mobile phase consisted of 0.5 mM H_2SO_4 with a flow rate of 0.6 mL min^{-1}, resulting in a retention time of 17.65 min for acetate anion (Fig. 9D). A calibration curve, linear from 5.0 mg L^{-1} to 100 mg L^{-1} ($R^2 = 0.9998$), was used for quantification. The method had a limit of detection (LOD) of 1.5 mg L^{-1} and a recovery efficiency of 98.4%. Samples were diluted 50-fold with the mobile phase and filtered (0.45 μm) prior to IC analysis. The acetic acid concentration determined by IC was consistent with the titration results. This crucial data provides further evidence confirming the near-complete release of CH_3COOH from the HDES 4 system into the aqueous phase immediately following extraction. This finding is entirely consistent with the ^{1}H-NMR data analyzed above, helping to elucidate the release mechanism of the extraction process.

Based on the presented data, it can be inferred that when HDES 4 interacts with an aqueous phase containing $HCrO_4^-$, the HDES 4 molecules at the solvent interface undergo an ion exchange process between Br^- and $HCrO_4^-$. Concurrently, the CH_3COOH molecules preferentially form hydrogen bonds with water molecules, leading to the breakdown of the HDES 4 structure and the complete release of the $[N8888]^+$ ion. This creates favorable conditions for the $HCrO_4^-$ ions to form an ionic bond with the $[N8888]^+$ ion, resulting in the formation of a new complex, [N8888][$HCrO_4$], while releasing the CH_3COOH molecules from their association with the HBA. Additionally, the ^{1}H-NMR spectra of HDES 4-Cr(VI) and HDES 4 after extraction do not exhibit signals corresponding to the COOH proton. Notably, the ^{1}H-NMR spectrum of HDES 4 after extraction closely resembles that of the original [N8888]Br. This represents an intriguing and novel finding. Previous study by Dong *et al.*[44] has demonstrated that DES systems remain intact during Cr(VI) extraction. Similarly, in our earlier work,[45] DESs formed from fatty acids maintained their structure after multiple extraction cycles. The key difference in this study is the use of acetic acid, a highly polar compound with excellent water solubility, which likely facilitates the complete release of the HBD molecules from the DES system. In summary, the mechanism of Cr(VI) extraction and regeneration by HDES 4 can be described by the following equation:

$$[N8888]Br\ldots(CH_3COOH)_4 + HCrO_4^- \rightleftarrows [N8888][HCrO_4^-] + 4CH_3COOH + Br^-$$

$$[N8888][HCrO_4] + KBr \rightleftarrows [N8888]Br + HCrO_4^-$$

3.6. Enrichment factor and application to real samples

3.6.1. Enrichment factor. The minimum concentration and enrichment factor are critical parameters for evaluating the efficiency of pollutant extraction.[62] In this study, the enrichment factor of Cr(VI) was assessed by adding 100 mg of DES to 10 mL standard solutions of Cr(VI) at a concentration of 0.50 mg L^{-1}. The mixture was shaken for 10 min at 500 rpm, after which the aqueous phase was discarded. This process was repeated nine more times to ensure maximum extraction. The extracted DES phase was then dissolved in acetonitrile and adjusted to a final volume of 10.0 mL. To determine the concentration of Cr(VI) in the enriched solution, a 0.1 mL aliquot was pipetted, followed by the addition of acid and DPC reagent. The solution was then diluted to the 50 mL mark, and the optical density was measured at 540 nm. The enrichment factor was calculated using eqn (5), 868 times, highlighting its high potential for the extraction and enrichment of Cr(VI) from dilute aqueous solutions. The high enrichment factor achieved in this study underscores the effectiveness of DES in extracting and concentrating Cr(VI), making it a promising candidate for applications in water treatment and pollutant removal. This method not only enhances the efficiency of Cr(VI) extraction but also provides a practical approach for handling low-concentration pollutants in environmental samples. The present study is compared with other published research on the solvent extraction of Cr(VI) using different solvents, as shown in Table 5. Previous studies have used traditional solvents such as dichloromethane, benzene, and toluene, often combined with large volumes of synergistic extractants.[63,64] In this work, a small amount of solvent was employed, resulting in an enrichment factor of over 83 times per cycle. When the extraction process is repeated over 10 consecutive cycles, the overall enrichment factor can reach up to 868 times. Additionally, the method is simple, fast, and can be performed with standard laboratory equipment.

3.6.2. Application to real samples analysis. The proposed extraction procedure was applied to real samples, including wastewater and drinking water. For wastewater samples, after filtration, 85% H_3PO_4 was added to adjust the pH to 1–2. A standard Cr(VI) solution was then introduced to achieve final concentrations of 0.2, 0.5, and 1.0 mg L^{-1}. Specifically, 100 mL of the water sample was transferred to a 100 mL volumetric flask, and precise volumes of 0.20 mL, 0.50 mL, and 1.00 mL of a 500 mg L^{-1} Cr(VI) standard solution were added to the respective flasks. For the extraction process, exactly 10.0 mL of the spiked sample was pipetted into vials, and 0.10 g of DES was added. The phases were then separated under the previously optimized conditions. After phase separation, the organic phase was dissolved in acetone, followed by the addition of 0.50 mL of phosphoric acid solution and 0.25 mL of DPC reagent. The mixture was allowed to stand until complete color development and then diluted to the mark with acetonitrile in a 50 mL volumetric flask. The experiment was conducted in triplicate, and the absorbance was measured at 540 nm.

The results, summarized in Table 6, reveal that even for complex real-world samples containing various components,

Table 5 Comparison of the proposed method *versus* other reported methods for Cr(VI) extraction[a]

Type of solvents	Instrument	Extraction technique/duration/amount of solvent	LOD, LOQ	RSD	EE, %	EF	Ref.
Benzene, toluene	UV-vis	Synergistic extraction (TBAB, TEA, TBP), 5.0 min with 10 mL of organic phase			98		64
Chloroform	UV-vis	EA-DLLME, 400 μL $CHCl_3$, 750 μL $NaHCO_3$ 2 M, 750 μL H_2SO_4 3M	0.001 mg L^{-1} 0.005 mg L^{-1}	<6.5%	83.0–117.6	21.4	63
DES: menthol, formic acid and acetic acid (1 : 1 molar ratio)	UV-vis	EA-DES DLLME, pH 4, 500 μL Na_2CO_3 2 M, 1000 μL CH_3COOH 2 M; 6 min	3 μg L^{-1} 10 μg L^{-1}	≤3.3% (intra-day)	81.1 −111.2	13.52	65
DMC	UV-vis	Synergistic with TBAB, 10 min, with 400 mg TBAB + 10 mL of organic phase			98		66
DES: ChCl-phenyl ethanol	FAAS	AA-EME-LD-DES, a 100 μL glass syringe for 9 cycles, with 250 μL DES, centrifuged for 4.0 min	LOD = 0.4 ng mL^{-1}	4.7%	95	39	67
DES: ChCl-phenol	GF-AAS	CFS-ME, centrifuged for 10 min, with 0.5 mL of THF + 59 μL DES	0.096 μg L^{-1}, 0.162 μg L^{-1}	4.1%	95.6	150	68
DES: ChCl, TBAC, TOMAC-phenol, decanoic acid	FAAS	UA-LLME, 0.4 mL THF + 0.4 mL DES	0.8 μg L^{-1} 3.2 μg L^{-1}	<5.0%		50	69
DES: TOMAC-parabens	UV-vis	LLME, vortexed for 3 min, centrifuged for 5 min, 0.10 g DES		≤4.1%	90	70	46
HDES: trioctylmethylammonium bromide-palmitic acid	UV-vis	LLME, vortexed for 3 min, centrifuged for 5 min, 0.10 g DES	0.023 mg L^{-1}, 0.077 mg L^{-1}	4.9%	96.5	83–93	45
HDES: tetraoctylammonium bromide- acetic acid	UV-vis	LLME, shaken for 10 min, 0.10 g DES	0.03 mg L^{-1} 0.1 mg L^{-1}	≤3.9%	>95	83–95	Present work

[a] ChCl: choline chloride, TEA: triethylamine, DMC: dichloromethane, TOA: trioctylamine, TBP: tetra butyl phosphate, TBAB: tetrabutylammonium bromide, TBAC: tetrabutylammonium chloride, TOMAC: trioctylmethylammonium chloride: THF: tetrahydrofuran, AA-EME-LD-DES: air agitated-emulsification microextraction-low density-deep eutectic solvent; CFS-ME: continuous flow sample microextraction, UA: ultrasound-assisted, LLME: liquid–liquid micro extraction, EA-DES DLLME: effervescent-assisted deep eutectic solvent-based dispersive liquid–liquid microextraction.

Table 6 Extraction of Cr(VI) in actual samples using HDES 4 ($n = 3$)[a]

Samples	Initial conc. Cr(VI) (mg L^{-1})	Added of Cr(VI) (mg L^{-1})	Conc. Cr(VI) in HDES 4 (mg L^{-1})	EE, %	EF, times
M1	0.00	1.0	81.2 ± 2.0	85.18 ± 0.60	81
		2.5	210.8 ± 6.9	94.31 ± 0.76	84
		5.0	412.6 ± 8.1	92.53 ± 4.58	82
M2	0.00	1.0	86.4 ± 2.1	86.35 ± 2.19	86
		2.5	217.5 ± 4.1	97.00 ± 0.44	87
		5.0	422.1 ± 3.4	94.42 ± 1.91	84

[a] M1: wastewater (pH 2.3, TSS 150 mg L^{-1}, conductivity > 2000 μS cm^{-1}, COD 100 mg L^{-1}, Fe^{3+} 1.5 mg L^{-1}, Ni^{2+} 0.6 mg L^{-1}, SO_4^{2-} 3.6 mg L^{-1}, NO_3^- 25.8 mg L^{-1}). M2: drinking water (pH 7, TDS < 50 mg L^{-1}, conductivity 0.055 μS cm^{-1}).

the enrichment factor consistently reaches 81–87 times, with extraction efficiencies exceeding 85%. This demonstrates that the proposed method exhibits high stability and sensitivity, making it suitable for application across a diverse range of sample matrices. However, to extend its applicability to other matrices such as food or geological samples, further investigations are required to provide a comprehensive understanding and broaden the method's scope.

3.7. Greenness assessment score

The greenness of the proposed Cr(VI) extraction method using HDES 4 was evaluated *via* the AGREE protocol,[70] yielding a high analytical greenness score of 0.76 (see detailed results in Fig. S3). This places the method in the upper range of the AGREE scale, indicating a relatively good level of analytical greenness. The high score reflects the method's proficiency in safe and straightforward sample preparation, as evidenced by elevated scores for criteria such as "Sample treatment," "Sample prep stages," and "Operator's safety," demonstrating alignment with established green chemistry principles. Specifically, the method excels in areas such as energy conservation during analytical processes (Score: 1.0), avoidance of derivatization (Score: 1.0), minimization of energy use (Score: 1.0), preference for reagents from renewable sources (Score: 1.0), and elimination of toxic reagents (Score: 1.0). The high scores for multi-analyte methods (0.84) and automation (0.75) are also contributing factors to the overall analytical greenness of the proposed method.

However, the assessment also reveals areas for significant improvement. The complete absence of *in situ* measurements (Score: 0.0) highlights a reliance on conventional sample preparation techniques that warrant refinement. Addressing this limitation is crucial, as *in situ* analysis eliminates sample transport and preparation steps, drastically reducing the environmental impact and potential for measurement inconsistencies related to device positioning, sample amount, and minimal sample size. Furthermore, while reagent sourcing and toxicity are adequately addressed, the relatively low scores for minimal sample size (0.32) and waste generation (0.39) necessitate further improvements in the method's overall environmental profile.

Therefore, to elevate the greenness score and enhance the sustainability of the method, several key improvements are warranted. These include: (1) the development of semi-automated sample processing procedures to improve efficiency and reduce waste; (2) the implementation of direct on-site analysis capabilities, exploring the potential of portable sensors or adapting the method for direct field application; and (3) an increase in the number of samples processed per batch to improve throughput. Crucially, a critical focus should be placed on investigating and implementing *in situ* measurement techniques, which have the potential to significantly reduce sample preparation steps and, consequently, improve the method's greenness. Addressing these areas will contribute to enhanced reliability, scalability, and an improved overall greenness score in future applications, leading to a more sustainable and practical analytical approach for Cr(VI) remediation.

4. Conclusion

In this study, a novel hydrophobic deep eutectic solvent based on tetraoctylammonium bromide and acetic acid was successfully synthesized and applied for the highly efficient removal of Cr(VI) from aqueous solutions. Under optimized conditions, the method achieved extraction efficiencies exceeding 95% across a broad pH range (2–10), demonstrating remarkable robustness. Kinetic and thermodynamic analyses revealed that the extraction process followed the pseudo-second-order model and was both spontaneous and endothermic. Mechanistic investigations, supported by ^{1}H-NMR and SEM-EDX, confirmed an ion-exchange mechanism facilitated by the release of the ammonium cation from the HDES structure. Furthermore, the method demonstrated excellent practical applicability with high enrichment factors (81–87 fold) in real wastewater matrices. With an AGREE greenness score of 0.76, this approach offers a sustainable, low-toxicity alternative to conventional solvent extraction. These findings suggest that acetic acid-based HDESs represent a promising platform for the development of green separation technologies in environmental remediation.

Author contributions

T.N. Huynh: investigation, data curation, formal analysis, validation. D.T. Nguyen: investigation, data curation, formal analysis. H.H.P.U. Pham: investigation, data curation, formal analysis. A.D. Trinh: conceptualization, data curation, methodology, software. Q.H. Tran: conceptualization, methodology,

writing – original draft, visualization, writing – review & editing, supervision.

Conflicts of interest

The authors of this paper state that they have no competing financial interests or personal relationships that could have influenced the reported work.

Data availability

All data supporting the findings of this study are available within the article and its supplementary materials. Raw data, including experimental protocols, analytical results, and characterization data, are available from the corresponding author upon reasonable request.

Supplementary information (SI) is available. See DOI: https://doi.org/10.1039/d5ra08693k.

References

1 D. T. Nguyen, H. N. Nguyen, T. M. Nguyen, H. C. Dong, N. N. Dang, Q.-H. Tran, T. A. Nguyen, M. Van Tran, T. Le Hoang Doan, L. C. Luu and M. Van Nguyen, *Colloids Surf., A*, 2024, **689**, 133663.
2 N. Van Cuong, T. Q. Hieu, P. T. Thien, L. D. Vu and L. Van Tan, *Rasayan J. Chem.*, 2017, **10**, 1446–1454.
3 V.-D. Doan, T. Q. N. Vo, H. P. Dang, T. L. H. Nguyen, Q.-H. Tran, A. T. Nguyen, V. A. Tran and V. T. Le, *Mater. Today Commun.*, 2024, **41**, 110678.
4 H. T. Nguyen, V.-D. Doan, T. L. Huong Nguyen, A.-T. Nguyen, Q.-H. Tran, V. A. Tran and V. T. Le, *RSC Adv.*, 2025, **15**, 6241–6259.
5 A. D. S. Oliveira, A. Bodo, T. M. Beltramini Trevilato, A. M. Magosso Takayanagui, J. L. Domingo and S. I. Segura-Muñoz, *Environ. Sci. Pollut. Res.*, 2007, **14**, 483–489.
6 M. S. Hossain, M. A. Shenashen, M. E. Awual, A. I. Rehan, A. I. Rasee, R. M. Waliullah, K. T. Kubra, Md. S. Salman, Md. C. Sheikh, Md. N. Hasan, Md. M. Hasan, A. Islam, Md. A. Khaleque, H. M. Marwani, K. A. Alzahrani, A. M. Asiri, M. M. Rahman and Md. R. Awual, *Process Saf. Environ. Prot.*, 2024, **185**, 367–374.
7 A. I. Rasee, E. Awual, A. I. Rehan, M. S. Hossain, R. M. Waliullah, K. T. Kubra, Md. C. Sheikh, Md. S. Salman, Md. N. Hasan, Md. M. Hasan, H. M. Marwani, A. Islam, Md. A. Khaleque and Md. R. Awual, *Surf. Interfaces*, 2023, **41**, 103276.
8 Md. C. Sheikh, Md. M. Hasan, Md. N. Hasan, Md. S. Salman, K. T. Kubra, M. E. Awual, R. M. Waliullah, A. I. Rasee, A. I. Rehan, M. S. Hossain, H. M. Marwani, A. Islam, Md. A. Khaleque and Md. R. Awual, *J. Mol. Liq.*, 2023, **389**, 122854.
9 A. Islam, S. Roy, M. A. Khan, P. Mondal, S. H. Teo, Y. H. Taufiq-Yap, M. T. Ahmed, T. R. Choudhury, G. Abdulkreem-Alsultan, S. Khandaker and Md. R. Awual, *J. Mol. Liq.*, 2021, **338**, 116703.
10 Md. T. Hossain, S. Khandaker, M. M. Bashar, A. Islam, M. Ahmed, R. Akter, A. K. D. Alsukaibi, Md. M. Hasan, H. M. Alshammari, T. Kuba and Md. R. Awual, *J. Mol. Liq.*, 2022, **368**, 120810.
11 T. L. DesMarias and M. Costa, *Curr. Opin. Toxicol.*, 2019, **14**, 1–7.
12 N. Sharma, K. K. Sodhi, M. Kumar and D. K. Singh, *Environ. Nanotechnol., Monit. Manage.*, 2021, **15**, 100388.
13 S. Prasad, K. K. Yadav, S. Kumar, N. Gupta, M. M. S. Cabral-Pinto, S. Rezania, N. Radwan and J. Alam, *J. Environ. Manage.*, 2021, **285**, 112174.
14 L. Van Tan, T. Quang Hieu and N. Van Cuong, *J. Anal. Methods Chem.*, 2015, **2015**, 1–7.
15 A. Monga, A. B. Fulke and D. Dasgupta, *J. Hazard. Mater. Adv.*, 2022, **9**, 100113.
16 P. Sharma, S. P. Singh, S. K. Parakh and Y. W. Tong, *Bioengineered*, 2022, **13**, 4923–4938.
17 P. Sharma, S. P. Singh, S. K. Parakh and Y. W. Tong, *Bioengineered*, 2022, **13**, 4923–4938.
18 J. K. Sueker, in *Environmental Forensics*, Elsevier, 1964, pp. 81–95.
19 US EPA (US Environmental Protection Agency), *Data Summary of the Third Unregulated Contaminant Mon-itoring Rule (UCMR 3). EPA 815-S-17-001*, USEPA, Washington, 2024.
20 I. Moffat, N. Martinova, C. Seidel and C. M. Thompson, *J. AWWA*, 2018, **110**(5), E22–E35.
21 T. Baskaran, *Water, Air, Soil Pollut.*, 2025, **236**, 603.
22 D. T. Nguyen, K. M. V. Nguyen, H. K. Duong, B. T. Nguyen, M. D. K. Nguyen, D. B. Tran, Q. H. Tran, T. L. H. Doan and M. V. Nguyen, *Dalton Trans.*, 2024, **53**, 7213–7228.
23 M. A. Islam, M. J. Angove, D. W. Morton, B. K. Pramanik and M. R. Awual, *J. Environ. Chem. Eng.*, 2020, **8**(2), 103515.
24 H. Peng and J. Guo, *Environ. Chem. Lett.*, 2020, **18**, 2055–2068.
25 D. A. Gkika, A. K. Tolkou, I. A. Katsoyiannis and G. Z. Kyzas, *Sep. Purif. Technol.*, 2025, **368**, 132996.
26 S. Imdad, R. K. Dohare, M. Agarwal and A. Srivastava, *Sep. Purif. Technol.*, 2023, **327**, 124908.
27 S. K. Singh and A. W. Savoy, *J. Mol. Liq.*, 2020, **297**, 112038.
28 A. P. Abbott, D. Boothby, G. Capper, D. L. Davies and R. K. Rasheed, *J. Am. Chem. Soc.*, 2004, **126**, 9142–9147.
29 Q. Zhang, K. De Oliveira Vigier, S. Royer and F. Jérôme, *Chem. Soc. Rev.*, 2012, **41**, 7108–7146.
30 W.-J. Huang, T. H. Vo, Y.-J. Sheng and H.-K. Tsao, *J. Mol. Liq.*, 2024, **396**, 124011.
31 A. Prabhune and R. Dey, *J. Mol. Liq.*, 2023, **379**, 121676.
32 T. C. Dung, T. Q. Hieu and L. Van Tan, *J. Food Compos. Anal.*, 2025, **147**, 108039.
33 H.-Y. Chi, H.-K. Tsao and Y.-J. Sheng, *J. Phys. Chem. B*, 2025, **129**, 5779–5787.
34 X. Liu, M. Chen, Z. Meng, H. Qian, S. Zhang, R. Lu, H. Gao and W. Zhou, *J. Chromatogr. B:Anal. Technol. Biomed. Life Sci.*, 2020, **1140**, 121995.
35 C. Florindo, L. C. Branco and I. M. Marrucho, *Fluid Phase Equilib.*, 2017, **448**, 135–142.
36 T. T. Nguyen, D. V. Nguyen, Q. H. Tran, M. D. Pham, V. M. Nguyen, T. T. Nguyen, C. D. Tran and T. D. Nguyen, *J. Mol. Liq.*, 2024, **397**, 124107.

37 F. Bu, Y. Zhao, B. Li, X. Zhang and J. Li, *Sustainable Chem. Pharm.*, 2023, DOI: 10.1016/j.scp.2023.101000.
38 M. J. Roldán-Ruiz, M. L. Ferrer, M. C. Gutiérrez and F. del Monte, *ACS Sustain. Chem. Eng.*, 2020, **8**, 5437–5445.
39 S. Wang, Z. Zhang, Z. Lu and Z. Xu, *Green Chem.*, 2020, **22**, 4473–4482.
40 P. D. OLA, Y. KUROBE and M. MATSUMOTO, *Solvent Extr. Res. Dev., Jpn.*, 2022, **29**, 31–37.
41 A. Shishov, S. Savinov, N. Volodina, I. Gurev and A. Bulatov, *Microchem. J.*, 2022, **179**, 107456.
42 J. Ali, M. Tuzen, D. Citak, O. D. Uluozlu, D. Mendil, T. G. Kazi and H. I. Afridi, *J. Mol. Liq.*, 2019, **291**, 111299.
43 W. Sapyen, J. Jirattisak, N. Bhawawet, N. Praphairaksit and A. Imyim, *Microchem. J.*, 2024, **202**, 110841.
44 H. Dong, E. Ci, T. Zhao, P. Chen, F. Liu, G. Hu and L. Yang, *Sep. Purif. Technol.*, 2024, **334**, 126104.
45 T. N. Huynh, T. T. Nguyen, C. D. Tran, Q. T. Nguyen, H. T. Nguyen, A. D. Trinh and Q. H. Tran, *J. Mol. Liq.*, 2025, **442**, 126954.
46 Y. Shi, D. Xiong, Y. Zhao, T. Li, K. Zhang and J. Fan, *Chemosphere*, 2020, **241**, 125082.
47 R. Liu, J. Hao, Y. Wang, Y. Meng and Y. Yang, *J. Mol. Liq.*, 2022, **365**, 120200.
48 H. Dong, E. Ci, T. Zhao, P. Chen, F. Liu, G. Hu and L. Yang, *Sep. Purif. Technol.*, 2024, **334**, 126104.
49 Q. Zheng, F. Yang, Q. Sun, H. Tan and X. Wang, *J. Mol. Liq.*, 2024, **410**, 125639.
50 S. Sowmiah, V. Srinivasadesikan, M.-C. Tseng and Y.-H. Chu, *Molecules*, 2009, **14**, 3780–3813.
51 T. Costa, Y. Sanchez-Vicente, Z. Yang, L. A. Stevens, F. de S. Dias and S.-C. Costa Pereira, *RSC Adv.*, 2024, **14**, 26246–26258.
52 Q. H. Tran, V. T. Le and V. C. Nguyen, *J. Chem.*, 2016, **2016**, 1–6.
53 Md. A. Islam, M. J. Angove, D. W. Morton, B. K. Pramanik and Md. R. Awual, *J. Environ. Chem. Eng.*, 2020, **8**, 103515.
54 A. Kumar, A. Thakur and P. S. Panesar, *J. Ind. Eng. Chem.*, 2019, **70**, 394–401.
55 S. Nayak, K. Lovering and A. Uysal, *Nanoscale*, 2020, **12**, 20202–20210.
56 Q. H. Tran, N. T. Nguyen and Le Van Tan, *Asian J. Chem.*, 2010, **23**, 1716–1718.
57 T. E. Phelps, N. Bhawawet, S. S. Jurisson and G. A. Baker, *ACS Sustain. Chem. Eng.*, 2018, **6**, 13656–13661.
58 A. Kruve, R. Rebane, K. Kipper, M. L. Oldekop, H. Evard, K. Herodes, P. Ravio and I. Leito, *Tutorial Review on Validation of Liquid Chromatography-Mass Spectrometry Methods: Part II*, Elsevier B.V., 2015, vol. 870.
59 Md. N. Hasan, Md. S. Salman, Md. M. Hasan, K. T. Kubra, Md. C. Sheikh, A. I. Rehan, A. I. Rasee, M. E. Awual, R. M. Waliullah, M. S. Hossain, A. Islam, S. Khandaker, A. K. D. Alsukaibi, H. M. Alshammari and Md. R. Awual, *J. Mol. Struct.*, 2023, **1276**, 134795.
60 Md. M. Hasan, K. T. Kubra, Md. N. Hasan, M. E. Awual, Md. S. Salman, Md. C. Sheikh, A. I. Rehan, A. I. Rasee, R. M. Waliullah, Md. S. Islam, S. Khandaker, A. Islam, M. S. Hossain, A. K. D. Alsukaibi, H. M. Alshammari and Md. R. Awual, *J. Mol. Liq.*, 2023, **371**, 121125.
61 Md. R. Awual, Md. M. Hasan, J. Iqbal, Md. A. Islam, A. Islam, S. Khandaker, A. M. Asiri and M. M. Rahman, *J. Environ. Chem. Eng.*, 2020, **8**, 103591.
62 Y. Shi, D. Xiong, Y. Zhao, T. Li, K. Zhang and J. Fan, *Chemosphere*, 2020, **241**, 125082.
63 A. Kebede, G. Tilachew, G. Chirfa and A. Gure, *S. Afr. J. Chem.*, 2022, **76**, 127–133.
64 P. K. Saw, A. K. Prajapati and M. K. Mondal, *J. Mol. Liq.*, 2018, **269**, 101–109.
65 G. Aregay Shifera, T. Tadesse Beyene and A. Gure, *Bull. Chem. Soc. Ethiop.*, 2025, **39**, 1245–1256.
66 P. Venkateswaran and K. Palanivelu, *Sep. Purif. Technol.*, 2004, **40**, 279–284.
67 M. Fasihi, M. Rajabi, B. Barfi and S. M. Sajjadi, *Int. J. Environ. Anal. Chem.*, 2022, **102**, 4331–4343.
68 S. Fouladlou, H. Faraji, H. Shahbaazi, A. Moghimi and F. Azizinezhad, *Microchem. J.*, 2021, **162**, 105834.
69 F. Elahi, M. B. Arain, W. A. Khan, N. Shah and T. G. Kazi, *Chem. Pap.*, 2021, **75**, 717–724.
70 F. Pena-Pereira, W. Wojnowski and M. Tobiszewski, *Anal. Chem.*, 2020, **92**, 10076–10082.